Session 6: System dynamics


l'été astro
Claire
MOUTOU

Tenth anniversary of 51 Peg-b : Status of and prospects for hot Jupiter studies
Proceedings of Haute Provence Observatory Colloquium (22-25 August 2005)
Edited by L. Arnold, F. Bouchy, and C. Moutou

Some open questions in the dynamics of extrasolar planetary systems

S. Ferraz-Mello[1], C. Beaugé[2], and T.A. Michtchenko[1]

[1] *Institute of Astronomy, Geophysics and Atmospherical Sciences, University of São Paulo, Brazil [sylvio@astro.iag.usp.br]*

[2] *Astronomical Observatory, National University of Cordoba, Argentina*

Abstract. The main concern of the dynamics of extrasolar planetary systems is the stability of the known systems and the identification of dynamical processes which may have determined their past evolution. It is expected that the systems will remain stable for times of the order of their age, but this question has to be answered for each system. These tasks are critically dependent on the access to the actual observational data. We identify immediate questions to be solved in order to determine the actual planetary masses (at least in units of the star mass), to understand the tidal evolution of close-in systems, as well as specific questions on the systems 47 UMa, 55 Cnc, HD 82943 and HD 160691, which could likely get better solutions if the modern techniques of Celestial Mechanics could be applied to the full sets of existing observations.

1. Introduction

In two recent papers (Beaugé et al. 2005a, Ferraz-Mello et al 2005a), the level of the gravitational interaction and the main resulting perturbations in the known extrasolar planetary systems was used to classify them. The known multi-planet systems were distributed into 3 classes, more or less according with the ratio of the orbital periods of planets in adjacent orbits. These ratios are directly related to the stability of the systems.

Class I includes planet pairs with small period ratio. A randomly constructed system with period ratio smaller than, say, 3 is likely to be unstable and short-lived. The observed systems with such small period ratio satisfy one of the two following conditions: (a) The planets are captured in resonant orbits; (b) The planets lie on almost circular orbits. The stability of these systems is critically dependent on the Keplerian orbital elements and a small uncertainty on their determination is enough to give rise to catastrophic events in the simulation of the systems (e.g the case of HD 82943; see Ferraz-Mello, Michtchenko & Beaugé 2005b).

The next class, class II, includes all other planet pairs in adjacent orbits with period ratio generally less than ~ 10. These planets show a significant dynamical interaction and usually present their periastra coupled in such a way that the difference of their longitudes, $\Delta\varpi$, oscillates about 0° or 180°. The stability in these cases is not so critically linked to the given Keplerian elements as in the previous case, but stability can be confirmed only if the orbits are reasonably well known. Possible instabilities can arise from the proximity to higher-order mean-motion resonances.

Finally, class III includes planets with larger period ratios (typically larger than ~ 30) and weak mutual interactions; these systems are very stable and even very inaccurate elements lead to stable solutions in numerical simulations; as a consequence, we cannot guess that the given elements of such systems are accurate or not just by looking at the results of simulations done using them.

To see updated orbital elements of the considered planetary systems see `http://www.astro.iag.usp.br/ dinamica/ exosys.htm`.

2. Class I planet pairs

Class I is formed by two sub-classes according with the characteristic responsible for the stability of the system. In Class Ia, we put planet pairs in mean-motion resonance and, in Class Ib, systems whose planets lie on orbits with small eccentricity. Class Ia includes planet pairs in which at least one of the components moves on a very eccentric orbit ($e > 0.2$). These pairs are necessarily resonant (otherwise they develop instabilities in short time). They are, currently, the planets of the stars HD 82943, HD 128311, and the planet pairs b-c of the stars GJ 876 and 55 Cnc. An odd system in this class is the pair of planets in HD 202206, which has a period ratio ~ 5. However, according with Correia et al. (2005), these planets are resonant and show the basic dynamics of the other planets in this class. The characteristic difference in this case is the mass of the innermost body, $m \sin i \sim 17.5$, much larger than all others. This means that the probability is high that the object is a sub-dwarf star rather than a planet. It is kept in our lists since, from the dynamical point of view, it is irrelevant if the components of a system are planets or sub-dwarfs. Class Ib is characterized by small period ratio and small eccentricities. This class includes only one known example among extrasolar planetary systems around main sequence stars, but, in addition, it includes the system of planets discovered around the pulsar PSR B 1257+12 and the Solar System. 47 UMa and PSR B 1257+12 are very important systems because they belong to the same kinematical class as the planets of our Solar System and may have a similar dynamical story. It is true that the pulsar planets formed in an environment completely different of the planets orbiting around MS stars and this may be the origin of the small eccentricities of their orbits. Its understanding may give some clues to understand why the planet orbits in our Solar System – and the putative planets of 47 UMa – are so different of the other extrasolar planetary systems.

3. Class II (and Class III) planet pairs

Class II is formed by planets in orbits not so relatively close as in the typical cases of Class I, but, nevertheless, in adjacent orbits close enough to enhance the dynamical interaction among them. The best known example is given by the two outer planets of the system υ And, which show a very rich dynamics (Michtchenko & Malhotra, 2003, Michtchenko, Ferraz-Mello & Beaugé 2005). The stability of this system is related to the conservation of the angular momentum, which is directly responsible for the e-e coupling (and the e-I coupling if the planets are not in coplanar orbits). In absence of close approaches (that is, in absence of important variations of the semi-major axes), the eccentricities of planets in adjacent orbits show an important cyclic variation and are at anti-phase in these cycles so that when the eccentricity of one of them increases, the other decreases. When the decreasing one reaches zero, the other cannot continue to grow and, therefore, remains bounded. There is also the e-ϖ coupling, which is the fact that these maxima and minima generally occur close to the positions in which the semi-major axes are aligned or anti-aligned (see Michtchenko & Malhotra, 2004). However, the most visible feature in these systems is the kinematical behavior usually (and improperly) called "secular resonance, characterized by the oscillation of the apsidal lines of the two planets around a common direction so that $\Delta\varpi$ oscillates about 0° or 180° (both cases are normal modes of oscillation of the secu;ar equation and, thus, possible). They are the planets of the stars HD 108874, υ And, HD 37124, HD 169830, the pair e-b of 55 Cnc and the pair b-c of μ Ara (= HD 160691). The inclusion of υ And b among these planets deserves a comment. The periastron of its orbit oscillates about the apastron of υ And c (see Ferraz-Mello et al. 2005a); however, this behavior may be just an artifact due to the difficulties for determination of the longitude of the periastron of this planet even when powerful techniques are used (see Ford, Lystad and Rasio, 2005).

Finally, Class III includes those planet pairs for which the gravitational interaction among the planets in each pair is relatively weak and the given orbits are very stable. One system difficult to class is HD 168443. The two planets of this star, whose current data correspond to orbits showing features characteristic of the hierarchical systems of class III, have masses (multiplied by $\sin i$) equal to 7.7 and 16.9 times the mass of Jupiter; these masses are so large that we have to consider the possibility that improved orbital elements correspond to orbits showing significant gravitational interaction.

4. Some Open Questions

The main open question concerns the origin of the systems; if it was possible to find scenarios for the migration, eccentricity enhancement and capture into resonance, in the case of the planets of Class Ia (see Papaloizou, 2003), many questions remain to be completely answered, as the marked difference between systems of the classes Ia and Ib.

Another question concerns the stability of the discovered systems. It is believed that the age of the discovered systems is not very different from the age of the stars themselves, what means some Gyrs. It is also expected that the systems will remain stable for time spans of the same order. However, this question has to be answered for each system and many of them could be solved if the observations were made soon available to theoreticians. The dynamical studies deserve to be undertaken with the same level of competence shown in the observational work and the policy of keeping observations unpublished for long times should be revised.

4.1 The mass and inclination indetermination

One of the shortcomings of the systems for which only radial velocity observations are available is the impossibility of kinematical determination of the inclination of the plane of the motion over the sky tangent plane, which leads to the impossibility of knowing the actual masses of the planets. The detection of effects due to the mutual perturbations in the observations may allow independent determination of the planet masses. This has been already done for two of the planets of the pulsar PSR B 1257+12 and two planets of GJ 876. In the case of the pulsar planets, the proximity to the 3:2 resonance is responsible for large perturbations in the longitude of the 2 planets (similar to the Great Inequality of Jupiter-Saturn)(see Malhotra, 1993). The outer planets of GJ 876 have benefited of a long span of high quality observations allowing the differences between a pure Keplerian solution and N-body fittings to be detected (see Laughlin et al, 2005). Other planets could soon be the subject of similar results if the observational data of all sources become available. At this point, it is worth mentioning that one of the unknowns of the problem is the mass of the star. According with Allende Prieto & Lambert (1999), even in the best cases they are not known with a precision better than ~ 8 percent. In fact, the comparison of published masses obtained with different stellar models shows discrepancies up to $10 - 15$ percent. If N-body codes are used in a blind way, this inaccuracy will pervade the whole set of results. It is however easy to choose units such that all indeterminate elements are put together as functions of the gauge factors $\sqrt[3]{M_{star}} \sin i$ and do not impair the determination of the other elements (inclusively the mass ratio, if both planets are assumed coplanar) (Ferraz-Mello et al. 2005a).

4.2 Close-in planets

Close-in planets have a tidal interaction with the stars. As long as just one planet is considered, the classical formulae giving the bulk variation of energy and angular momentum are enough to model the evolution of one planet (see Pätzold et al. 2004). The great problem, here, is the choice of the Love numbers and the dissipation parameters of both the star and the planet. Furthermore, if the planet belongs to a system and if it has (or had) the possibility of being tied to another planet through a mean-motion resonance, bulk formulae can no longer be used because the averaged equations giving the gravitational evolution of the couple are not the same inside and outside the resonance. In such case, we need to consider the actual forces. In what concerns the tides raised by the planet on the rotating star we may use formulas corresponding to the second harmonic of the classical Darwin theory (see Mignard, 1981). However, the tides raised by the star on a close-in planet lead to its spin-orbit synchronization and the theory needs to be adapted to include the radial tides. An easy-to-work equation for these forces is not available. This question requests an urgent solution since the increasing discoveries of exoplanets by transits will soon lead to systems in which the interplay of tides and resonance will have to be taken into account to determine the evolution of the system. We remind that tidal effect on close-in planets is to drive the planet to star. In at least one case (the system HD 82943), there are evidences of the past engulfment of one planet in the star (Israelian et al. 2001).

Just for illustration, we show in Fig. 1 the plots of the semi-major axes and eccentricities of two planets initially in a 2:1 apsidal corotation resonance. The timescale is arbitrary since it depends on the values

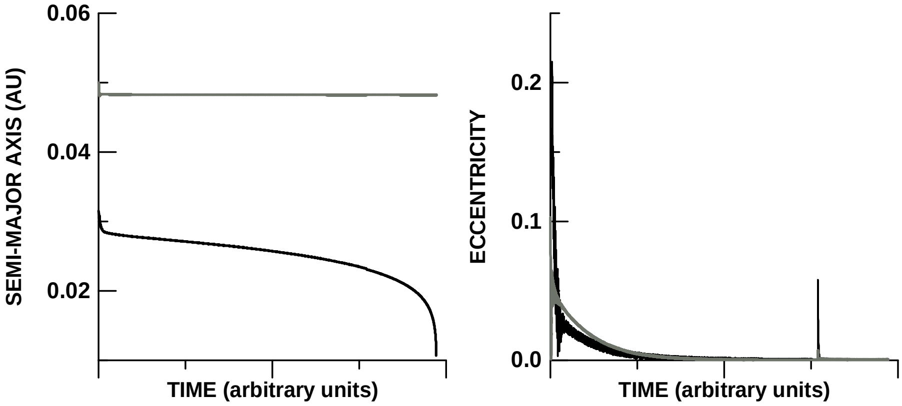

Figure 1. *Variation of the semi-major axes and eccentricities of a pair of planets, initially in 2:1 resonance, under the action of tidal interaction with the star.*

adopted for the tidal parameters of the star and the planet. It is typically of the order of 1 Gyr, but this number is inversely proportional to the dissipation factor Q and can be strongly affected by its change. The spike seen in the eccentricity plot of the inner planet is due to the enhancement of the eccentricity when the inner planet crosses, in its fall to the star, the 3:1 resonance.

4.3 Some specific questions (in order of priority)

47 UMa

The joint analysis of the observations from several observatories should be considered as a priority. 47 UMa is the only extrasolar system around a Main Sequence star with characteristics similar to the Solar System. However, the analysis of some series of observations cast a doubt on the existence of one of the planets in this pair (Naef et al, 2004). The joint analysis of the existing observation should help to solve this dilemma.

55 Cnc $= \rho$ *Cnc A*

The two intermediary planets of 55 Cnc are also the subject of doubts concerning the existence of one of them (55 Cnc c) (Naef, 2004). Assuming coplanar orbits, the published elements correspond to a resonant system whose motion is a large amplitude oscillation about a stationary solution (apsidal corotation resonance). The scenario of migration due to disk-planet interaction would be better compatible, in this case, with a solution closer to the stationary solution. However, the position of the stationary solution depends on the mass ratio of the two planets and a joint analysis of the existing observations should help not only to decide if 55 Cnc c indeed exists, but also, in that case, to check the small eccentricity attributed to 55 Cnc b and to provide a new estimation of the mass ratio. On the other hand, the influence of the companion star ρ Cnc B on the stability of the system remains to be considered.

HD 82943

The solutions obtained for this system range from solutions leading to catastrophic events in less than 100,000 years to solutions which remain stable forever (Mayor et al. 2004, Ferraz-Mello et al. 2005b). The contours of the stable regions is critically linked to the planet masses and a better mass determination is necessary to get a better map of them. The real state of motion of this system is an open question. In addition, there is the suspicion that this system had a catastrophic event in the past, with the fall of one planet on the star (Israelian et al 2001), and we cannot rule out the consequences of such an event on the dynamics of the remaining system. In this case, the improvement of the orbital elements depends on the realization of new and more accurate observations.

HD 160691 b,c

The problems of this system are similar to those found for HD 82943: solutions leading to catastrophic events in less than 100,000 years and solutions which remain stable forever, both fitting evenly the observations, were found (Gozdziewski, Konacki & Maciejewicz 2005). The problem of this system will not be solved soon because of the long periods of the planets involved (1.8 to 10 years). The stability maps show that even the stable solutions found are near the edge of the regular region indicating that the system is possibily being seen nearly edge-on (otherwise these orbits also would become unstable).

References

Allende Prieto, C. & Lambert, D.L. 1999, A&A352 , 555

Beaugé , C., Callegari Jr., N., Ferraz-Mello, S., & Michtchenko, T.A. 2005a, in *Dynamics of Populations of Planetary Systems* IAU Colloquium 197, eds. Z. Knezevic, & A. Milani, (Cambridge: Univ.Press) 3

Beaugé, C., Ferraz-Mello, S., & Michtchenko, T.A. 2005b, MNRAS (submitted) (astro-ph/0404166).

Correia, A.C.M., Udry, S., Mayor, M., Laskar, J., Naef, D., Pepe, F., Queloz, D., & Santos, N. C. 2005, A&A440, 751.

Ferraz-Mello, S., Michtchenko, T.A., Beaugé, C., & Callegari Jr., N. 2005a, In *Chaos and stability in Extrasolar Planetary Systems* ed. R. Dvorak et al., Lecture Notes in Physics, (Berlin: Springer) (in press).

Ferraz-Mello, S., Michtchenko, T.A., & Beaugé, C.. 2005b, ApJ621, 473

Ford, E.B., Lystad, V., & Rasio, F.A. 2005 Nature, 434, 873

Gozdziewski, K.. Konacki, M., & Maciejewicz, A. 2005, ApJ622, 1136

Israelian, G., Santos, N. C., Mayor, M., & Rebolo, R. 2001, Nature 411, 163

Laughlin, G., Butler, R.P., Fischer, D., Marcy, G.W., Vogt, S.S., & Wolf, A.S. 2005, ApJ622, 1182L

Malhotra, R. 1993, ApJ407, 266.

Mayor, M., Udry, S., Naef, D., Pepe, F., Queloz, D., Santos, N. C., & Burnet, M. 2004, A&A415, 391

Michtchenko, T. & Malhotra, R. 2004, Icarus 168, 237

Michtchenko, T., Ferraz-Mello, S., & Beaugé, C. 2005, Icarus (submitted) (astro-ph 0505169)

Mignard, F. 1981, Moon and Planets 20, 301

Naef, D., Mayor, M., Beuzit, J.L., Perrier, C., Queloz, D., Sivan, J.P., & Udry, S. 2004 A&A414, 351

Papaloizou, J.C.B. 2003, Celest. Mech. Dynam. Astron. 87, 53

Pätzold, M., Carone, L., & Rauer, H. 2004, A&A427, 1075

Tenth anniversary of 51 Peg-b : Status of and prospects for hot Jupiter studies
Proceedings of Haute Provence Observatory Colloquium (22-25 August 2005)
Edited by L. Arnold, F. Bouchy, and C. Moutou

On the relation between hot-Jupiters and the Roche limit

E. B. Ford[1] and F. A. Rasio[2]

[1] *Astronomy Department, UC Berkeley, 601 Campbell Hall, Berkeley, CA 94709, USA [eford@astro.berkeley.edu]*

[2] *Dept. of Physics & Astronomy, Northwestern, 2145 Sheridan Road, Evanston, IL 60208-834*

Abstract. Many of the known extrasolar planets are "hot Jupiters," giant planets with orbital periods of just a few days. We use the observed distribution of hot Jupiters to constrain the location of the "inner edge" and planet migration theory. If we assume the location of the inner edge is proportional to the Roche limit, then we find that this edge is located near twice the Roche limit, as expected if the planets were circularized from a highly eccentric orbit. If confirmed, this result would place significant limits on migration *via* slow inspiral. However, if we relax our assumption for the slope of the inner edge, then the current sample of hot Jupiters is not sufficient to provide a precise constraint on both the location and power law index of the inner edge.

1. Introduction

How about early radial velocity discoveries were interpreted as showing a pile-up at an orbital period of three days, but recent transit surveys and very sensitive radial velocity observations have discovered planets with even shorter orbital periods. These discoveries suggest that the inner edge for hot Jupiters is not defined by an orbital period, but rather by a tidal limit which depends on both the semi-major axis and the planet-star mass ratio (see Fig. 1). This would arise naturally if the inner edge were related to the Roche limit, the critical distance at which a planet fills its Roche lobe. The Roche limit, a_R is is defined by

$$R_P = 0.462 a_R \left(\frac{M_P}{M_*}\right)^{1/3} \tag{1}$$

where R_P is the radius of the planet, M_P is the mass of the planet, and M_* is the mass of the star. The numerous mechanisms proposed to explain the migration of giant planets to short period orbits can be divided into two broad categories:

i) Mechanisms involving slow inspiral, such as migration due to a gaseous disk or planetesimal scattering (Trilling et al. 1998, Gu et al. 2003). These would result in a limiting separation equal to the Roche limit.

ii) Mechanisms involving the circularization of highly eccentric orbits with small pericenter distances, possibility due to planet-planet scattering (Rasio & Ford 1996, Ford, Havlickova, & Rasio 2001, Papaloizou & Terquem 2001, Marzari & Weidenschilling 2002), secular perturbations from a wide binary companion (Holman, Touma, & Tremaine 1997), or tidal-capture of free-floating planets (Gaudi 2003). These would result in a limiting separation of *twice* the Roche limit (Faber et al. 2004).

2. Statistical Analysis

To quantitatively explore the observational constraints on the distribution of hot Jupiters, we employ the techniques of Bayesian inference. In the Bayesian framework, the model parameters are treated as random variables which can be constrained by the actual observations. Therefore, to perform a Bayesian analysis it is necessary to specify both the likelihood (the probability of making a certain observation given a particular set of model parameters) and the prior (the *a priori* probability distribution for the model parameters). Let us denote the model parameters by θ and the actual observational data by d, so that the joint probability distribution for the observational data and the model parameters is given by

$$p(d, \theta) = p(\theta)p(d|\theta) = p(d)p(\theta|d), \tag{2}$$

where we have expanded the joint probability distribution in two ways and both are expressed as the product of a marginalized probability distribution and a conditional probability distribution. The prior is given by $p(\theta)$ and the likelihood by $p(d|\theta)$. On the far right hand side, $p(d)$ is the *a priori* probability for observing the values actually measured and $p(\theta|d)$ is the probability distribution of primary interest, the *a posteriori* probability distribution for the model parameters conditioned on the actual observations, or simply the posterior. The probability of the observations $p(d)$ can be obtained by marginalizing over the joint probability density and again expanding the joint density as the product of the prior and the likelihood. This leads to Bayes' theorem, the primary

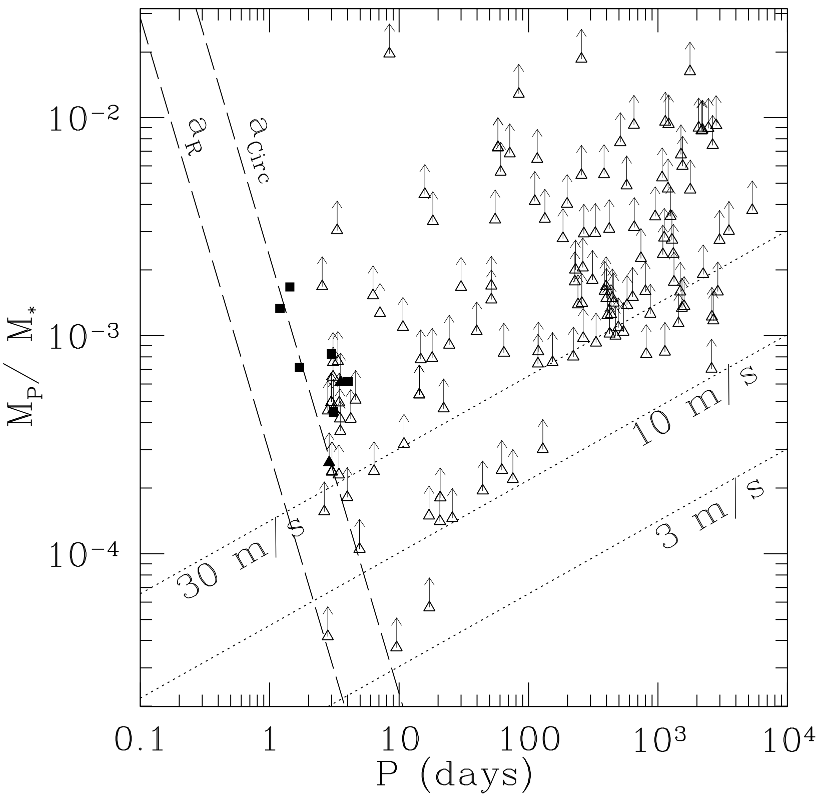

Figure 1. *Minimum mass ratio versus orbital period for the current observed sample of planetary companions. Planets discovered by radial velocity surveys are shown as triangles with arrows indicating* $1-\sigma$ *uncertainties in mass due to unknown inclination. The solid triangles have inclinations and radii measured via transits. The solid squares show planets discovered by transit searches. The dotted lines show the minimum mass corresponding to various velocity semi-amplitudes and roughly indicate where radial velocity surveys are nearly complete (*$\geq 30m/s$*), have significant sensitivity (*$\geq 10m/s$*), and are only beginning to detect planets (*$\geq 3m/s$*). The two dashed lines show the the location of the Roche limit (*a_R*) and the ideal circularization radius (*$a_{\rm circ}$*) for a planet with a radius,* $R_P = 1.2R_J$*. The inner edge for the distribution of hot Jupiters is near* $a_{\rm circ}$*. Note that the red lines do not apply to the lowest mass planets that likely have a radius significantly less than* $1.2R_J$ *due to their qualitatively different internal structure.*

tool for Bayesian inference,

$$p(\theta|d) = \frac{p(d|\theta)p(\theta)}{p(d)} = \frac{p(d|\theta)p(\theta)}{\int d\theta p(d|\theta)p(\theta)}. \tag{3}$$

Often the model parameters contain one or more parameters of particular interest (e.g., the location of the inner cutoff for hot Jupiters in our analysis) and other nuisance parameters which are necessary to adequately describe the observations (e.g., the fraction of stars with hot Jupiters in our analysis). Since Bayes' theorem provides a real probability distribution for the model parameters, we can simply marginalize over the nuisance parameters to calculate a marginalized posterior probability density, which will be the basis for making inferences about the location of the inner cutoff for hot Jupiters.

We construct models for the distribution of hot Jupiters and use Bayes' theorem to calculate posterior probability distributions for model parameters given the orbital parameters measured for extrasolar planets discovered by radial velocity surveys. For the sake of clarity, we start by presenting a simplistic one-dimensional model for the distribution of hot Jupiters. We then gradually improve our model to understand how each model improvement affects our results.

The primary question which we wish to address in this paper is the location of the inner edge of the distribution of hot Jupiters relative to the location of the Roche limit. Therefore, we define $x \equiv a/a_R$, where a is the semi-major axis of the planet and a_R is the Roche limit. We assume that the actual distribution of x for various hot Jupiters is given by a truncated power law,

$$p(x|\gamma, x_l, x_u)dx = x^\gamma \left(\frac{dx}{x}\right), \quad x_l < x < x_u, \tag{4}$$

and zero else where. Here γ is the power law index and x_l and x_u are the lower and upper limits for x. The lower limit, x_l, is the model parameter of primary interest, while γ and x_u are nuisance parameters. Therefore, our results are summarized by the marginalized posterior probability distribution for x_l.

In order to minimize complexities related to the analysis of a population, we choose to restrict our analysis to a subset of the known extrasolar planets for which radial velocity surveys are complete and extremely unlikely to contain any false positives. To obtain such a sample, we impose two constraints: $P \leq P_{\max}$, where $P_{\max}$ is the maximum orbital period, and $K \geq K_{\min}$, where $K_{\min}$ is the minimum velocity semi-amplitude. We use $K_{\min} = 30$m/s, based on the results of simulated radial velocity surveys (Cumming 2004). We typically set $P_{\max} =$ 30 days, even though radial velocity surveys are likely to be complete even for longer orbital periods (provided $K \geq K_{\rm min}$). This minimizes the chance of introducing biases due to survey incompleteness or possible structure in the observed distribution of planet orbital periods at larger periods. By considering only planets with orbital parameters such that radial velocity surveys are very nearly complete, our analysis does not depend on the velocities of stars for which no planets have been discovered. Note that our criteria for including a planet may introduce a bias depending on the actual mass-period distribution. We will address this point with a two-dimensional model at the end of our analysis. Also, our criteria exclude any planet discovered via techniques other than radial velocities (e.g., transits), even if subsequent radial velocity observations were obtained to confirm the planet.

Initially, we make several simplifying assumptions to make an analytic treatment possible. We assume uniform prior probability distributions for each of the model parameters, $p(\gamma) \sim U(\gamma_{\rm min}, \gamma_{\rm max})$ and $p(x_l, x_u) \sim$ const, provided $x_{ll} < x_l < x_u < x_{uu}$ and zero otherwise. The lower and upper limits (x_{ll} and x_{uu}) for each parameter are chosen to be sufficiently far removed from regions of high likelihood that the limits do not affect the results. We assume that the orbital period (P), velocity semi-amplitude (K), semi-major axis (a), stellar mass (M_*), and planet mass times the sin of the inclination of the orbit relative to the line of sight ($m \sin i$) are known exactly based on the observations.

We begin by assuming that $\sin i = 1$ for all planets and that all planets have the same radius, R_P. With these assumptions, the posterior probability distribution is given by

$$p(x_l, x_u, \gamma | x_1, ... x_n) \sim \gamma^n (x_u^\gamma - x_l^\gamma)^{-n} \prod_{j=1}^{n} x_j^{\gamma-1}, \tag{5}$$

provided that $x_{ll} < x_l \leq x_{(1)} \leq x_{(n)} \leq x_u < x_{uu}$ and $\gamma_{\rm min} < \gamma < \gamma_{\rm max}$. Here n is the number of planets included in the analysis, $x_{(1)}$ is the smallest value of x among the sample of hot Jupiters used in the analysis, and $x_{(n)}$ is the largest value of x in the sample. The normalization can be obtained by integrating over all allowed values of x_l, x_u, and γ.

We show the marginal posterior distributions in which we have integrated over the nuisance parameters, x_u and γ in Fig. 2 (left, dotted line), assuming $R_P = 1.2 R_J$. The distribution has a sharp cutoff at $x_{(1)}$ and a tail to lower values reflecting the chance that $x_l < x_{(1)}$ due to the finite sample size.

Next, we assume that the actual distribution of orbital inclinations is isotropic ($\cos i \sim U[-1, 1]$). For planets which were discovered by radial velocities and the inclination was subsequently determined with the detection of transits, we use the measured inclination. The marginal

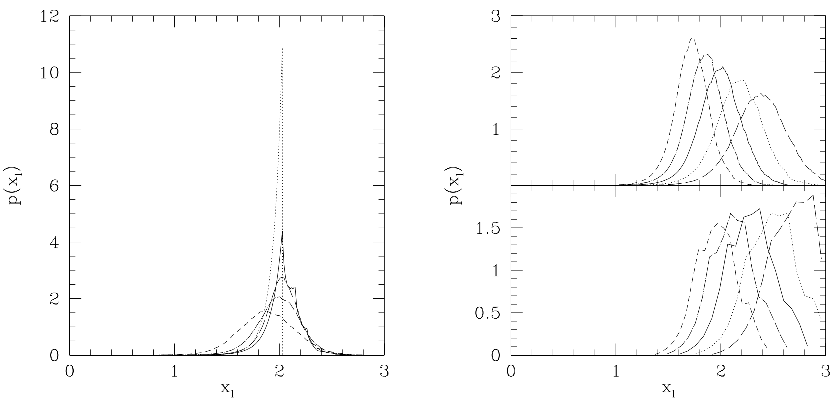

Figure 2. *Left: Marginal posterior distribution for x_l, the location of the inner edge for the population of hot Jupiters. The dotted line assumes all systems are viewed edge on ($\sin i = 1$). The solid line assumes an isotropic distribution of orbital inclinations (except for transiting planets). The remaining lines replace the assumption of $R = 1.2R_J$ for all non-transiting planets with a normal distribution for the planet radii using a dispersion dispersion of $\sigma_{R_P} = 0.05R_J$ (long dashes), $0.1R_J$ (dots-dashes), or $0.2R_J$ (short dashes). Upper Right: Dependence of the marginal posterior distribution for x_l on the assumed mean planet radius. $\langle R_P \rangle = 1.0R_J$ (long dashes), $1.1R_J$ (dotted), $1.2R_J$ (solid), $1.3R_J$ (dotted dashed), and $1.4R_J$ (short dashes), all assuming $\sigma_{R_P} = 0.1R_J$. Lower Right: Same as above, but using a 2-d model (period & mass) which accounts for selection effects.*

posterior distribution for x_l is shown in Fig. 2 (left, solid line). The sharp cutoff at $x_{(1)}$ is replaced with a more gradual tail, reflecting the chance that $\sin i < 1$ for planets with the smallest values of x.

Next, we consider the consequences of allowing for a distribution of planetary radii. For transiting planets we use a normal distribution for the radius based on the published radius and uncertainty. For non-transiting planets, we assume a normal distribution of planetary radii with standard deviation, σ_{R_P}. We show the resulting marginalized posterior distributions in Fig. 2 (left). Allowing for a significant dispersion broadens the posterior distribution for x_l and results in a slight shift to smaller values.

We have also explored the effects of varying the model parameter $P_{\max}$, exploring values from 8 to 60 days. We find that this does not make a discernible difference in the posterior distribution for x_l.

Our results are sensitive to our choice for the mean radius for the non-transiting planets. In Fig. 2 (upper right) we show the posterior distributions for various mean radii, assuming $\sigma_{R_P} = 0.1R_J$. Since few planets have a known inclination, there is a nearly perfect degeneracy between R_P and x_l. Even when we include transiting planets, this degeneracy remains near perfect, i.e., $p(x_l|R_p, x_1, ..., x_n) \simeq p(x_l \cdot \frac{R'_P}{R_P}|R'_P, x_1, ..., x_n)$. However, it can be seen that is extremely unlikely for x_l to be near unity for any reasonable planetary radius.

We have also performed an improved analysis using a two dimensional model which considers the joint planet mass-period distribution function. This allows us to account for observational selection biases due to the minimum mass for detecting a planet depending on the orbital period. We assume that the distribution function is a truncated power law in both planet-star mass ratio and period. That is

$$p(P, \mu|\alpha, \beta, P_{\min}P_{\max}, \mu_{\min}, \mu_{\max}, c) \sim cP^{\alpha}\mu^{\beta}\frac{dP}{P}\frac{d\mu}{mu}, \qquad (6)$$

provided $\mu_{\min} < \mu < \mu_{\max}$, $P < P_{\max}$, and $a(P, M_*) \geq x_l \cdot a_R(R_P, \mu)$. Here $\mu = M_P/M_*$, and α and β are the new power law indices. We find the marginal posterior distribution for x_l is very similar to the results of our 1-d analysis. The most significant difference is that the posterior distribution for x_l shifts slightly to wards *larger* separations (see Fig. 2, lower right).

3. Discussion

The current distribution of hot Jupiters discovered by radial velocity searches shows a cutoff that is a function of orbital period and planet mass. Our Bayesian analysis solidly rejects the hypothesis that the cutoff occurs inside or at the Roche limit, in contrast to what would be expected if the hot Jupiters had slowly migrated inwards on a circular orbit. Instead, our analysis shows that this cutoff occurs at a distance nearly twice that of the Roche limit, as expected if the hot Jupiters were circularized from a highly eccentric orbit. These findings suggest that hot Jupiters may have formed via planet-planet scattering (e.g., Rasio & Ford 1996), tidal capture of free floating planets (Gaudi 2003), or secular perturbations from a highly inclined binary companion (e.g., Holman, Touma, & Tremaine 1997). If the hot Jupiters indeed were circularized from a high eccentricity orbit, then this raises the challenge of explaining the origin of giant planets with orbital periods $\sim 10 - 100$ days.

An alternative explanation is that the planets migrated inwards on a nearly circular orbit at a time when the planets were roughly twice their current radii. Future observations of low mass planets may make it possible to test this alternative, assuming that the time evolution of their contraction is significantly different than for Jupiter-mass planets. A third alternative is that short-period giant planets are destroyed by another process before they reach the Roche limit. HST observations of HD 209458 indicate absorption by matter presently beyond the Roche lobe of the planet and have been interpreted as evidence for a wind leaving the planet powered by stellar radiation (Vidal-Madjar et al. 2003, 2004). Further theoretical work will help determine under what conditions these processes can cause significant mass loss.

Future planet discoveries will either tighten the constraints on the model parameters or provide evidence for the existence of planets definitely closer than twice the Roche limit. In particular, new discoveries of very low mass planets could better constrain the shape of the inner cutoff as a function of mass. In the future, an improved analysis could also include such low-mass planets where surveys are not yet complete. For future theoretical work, we hope to explore the possibility of orbital circularization occurring at larger orbital radii, possibly in a protoplanetary disk or while the star is young and still contracting.

Acknowledgements. We thank Eugene Chiang, Tom Loredo, Norm Murray, Ruth Murray-Clay, John Papaloizou, Frederic Pont for their comments. This research was supported by NSF grants AST-0206182 and AST0507727 at Northwester and a Miller Research Fellowship at UC Berkeley.

References

Cumming, A. 2004, MNRAS, 354, 1165

Faber, J.A., Rasio, F.A., & Willems, B. 2005, Icarus, 175, 248

Ford, E.B., Havlickova, M., & Rasio, F.A. 2001, Icarus, 150, 303

Gaudi, S. 2003, astro-ph/0307280

Gu, P.-G., Lin, D.N.C., & Bodenheimer P.H. 2003, ApJ, 558, 509

Holman, M., Touma, T., & Tremaine, S. 1997, Nature, 386, 254

Marzari, F., & Weidenschilling, S.J. 2002, Icarus 156, 670

Papaloizou, J.C.B., & Terquem, C. 2001, MNRAS, 325, 221

Rasio, F.A., & Ford, E.B. 1996, Science, 274, 954

Trilling, D. E., Benz, W., Guillot, T., *et al.* 1998, ApJ, 500, 428

Vidal-Madjar, A., Lecavelier des Etangs, A., Désert, J.-M., *et al.* 2003, Nature, 422, 143

Vidal-Madjar, A., Désert, J.-M., Lecavelier des Etangs, A., *et al.* 2004, ApJ Letters, 604, 69

Tenth anniversary of 51 Peg-b : Status of and prospects for hot Jupiter studies
Proceedings of Haute Provence Observatory Colloquium (22-25 August 2005)
Edited by L. Arnold, F. Bouchy, and C. Moutou

Gliese 86b – A close moving giant planet in a binary system

E. Pilat-Lohinger, B. Funk, and R. Dvorak

Institute for Astronomy, Vienna University, Türkenschanzstrasse 17, A-1180 Vienna, Austria [lohinger@astro.univie.ac.at]

Abstract. In our dynamical study we give a short insight into the stability of planetary motion in the binary Gliese 86AB, where a giant planet was discovered at about 0.11 AU. Further observations showed a sub-stellar companion, which is either a brown dwarf or a white dwarf. We compare the "two systems" and examine the influence of the "hot-jupiter" on the habitable zone of the K main-sequence star Gliese 86A.

1. Dynamical stability study of Gliese86

Gliese 86AB is a close binary system, where a giant planet ($M \sin(i) = 4M_{Jupiter}$) was detected at about 0.11 AU from the K1 V star with a period of less than 16 days (Queloz et al. 2000). Further observations by Els et al. (2001) using the ESO adaptive optic system ADONIS showed a sub-stellar companion – a brown dwarf (BD) of $\sim 50M_{Jupiter}$ at about 18.75 AU. Very recently, this binary system was observed by Mugrauer & Neuhäuser (2005) using NAOS-CONICA (NACO) and its new Simultaneous Differential Imager (SDI) as well as NACO spectroscopy, from which they concluded that the secondary should be a white dwarf (WD) of at least 0.55 solar-masses.
In our dynamical study of this binary we compare the planetary motion around Gliese 86A for both configurations. For the computations we used the orbital parameters given by the observations and determined the dynamical state of the orbits by means of (i) the Fast Lyapunov Indicator (FLI), a well known chaos indicator (Froeschlé et al. 1997), and (ii) the maximum eccentricity (MEC) which is very important for studies in the habitable zone (HZ) – i.e. the region around a sun-like star where we can expect similar conditions for a planet like on our Earth. We studied the influence of Gliese 86b on the HZ of Gliese 86A by means of the MEC.

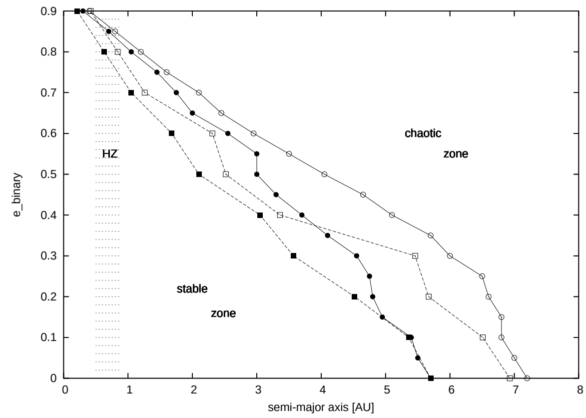

Figure 1. *Stability map for a test-planet in the binary Gliese 86AB, where the detected planet at 0.11 AU was neglected. We show the three zones (stable/mixed/chaotic) for the two configurations (dashed lines with open and full squares for a WD and the full lines with open and full circles are those for a BD).*

2. Results

For the general stability study we used the restricted 3-body problem (RTBP), where the "mass-less test-planet" moves in the gravitational field of the binary Gliese 86AB and the detected planet is neglected. We study both orbital configurations – a BD or a WD as secondary. The computations were carried out for 100000 periods of the binary, where we determined the dynamical state of the orbits by means of the FLI. All test-planets were started in circular motion at semi-major axes between 0.3 and 9 AU with a step of 0.01 AU. Since the eccentricity of the binary is not determined from the observations yet, we define the stable zone for planetary motion for all e_{binary} (from 0. to 0.9). A corresponding stability map (semi-major axis versus e_{binary}, Figure 1) shows 3 zones: (i) a *stable zone* whose border is defined by the largest distance from Gliese 86A up to which we have found only regular motion; (ii) a *mixed zone*, which is in-between the border-line, where both regular and chaotic motion can be found and (iii) a *chaotic zone* with only chaotic motion. The results show that for circular and low eccentric motion ($e_{binary} = 0.1$) the border-lines for the two systems are nearly at the same positions, while for higher eccentricities of the binary both border-lines are closer to Gliese 86A, if the secondary is a white dwarf. In the second part of our investigation, we studied the stability of fictitious planets in the HZ of Gliese 86A, which was carried out for two eccentricities of the binary (0.2 and 0.7). For the long-term stability we computed the FLIs. To see the influence of the detected planet Gliese

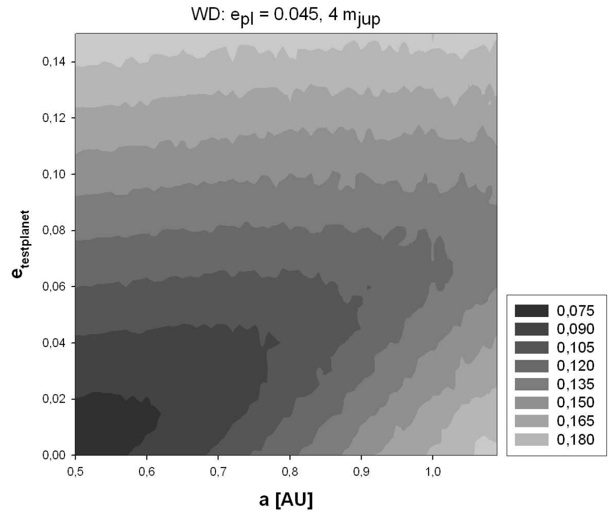

Figure 2. *MEC plot of the HZ for the real configuration, when the secondary is a WD and $e_{binary} = 0.7$. The grey scaling shows the different MEC values – from 0.06 (darkest region) to 0.18 (brightest region) the influence of the secondary is given by the higher MEC values in the bottom right corner of the plot.*

86b and of the secondary, we calculated the maximum eccentricities over 100000 years. The MEC-plot (Figure 2) represents the region of the HZ (x-axis) for different initial eccentricities of the test-planets (y-axis), where the gray-scaling shows the different MEC values. To see also an influence of the secondary, we show one of the plots for $e_{binary} = 0.7$. The parameters for the detected planet were varied in the following way: (i) as mass we used the minimum mass ($4M_{Jupiter}$) and the double ($8M_{Jupiter}$) and (ii) as eccentricity we used 0.045 (as determined from the observation) up to 0.15. As an example, we show in Figure 2 the result for the configuration given by Mugrauer & Neuhäuser (2005). A more detailed study thereto is already in preparation.

Acknowledgements. The authors wish to acknowledge the support by the Austrian FWF (EP-L: Hertha Firnberg Project T122 and BF: Project P16024-TPH). This study was also supported by the International Space Science Institute (ISSI) and benefits from the ISSI team "Evolution of Habitable Planets".

References

Queloz, D., Mayor, M., Weber, L. et al. 2000, A&A, 354, 99
Els, S.G., Sterzik, M.F, Marchis, F. et al. 2001, A&A, 370, L1
Mugrauer, M., & Neuhäuser, R. 2005, MNRAS, 361, L15
Froeschlé, C., Lega, E., & Gonczi, R. 1997, CMDA, 64, 21

Tenth anniversary of 51 Peg-b : Status of and prospects for hot Jupiter studies
Proceedings of Haute Provence Observatory Colloquium (22-25 August 2005)
Edited by L. Arnold, F. Bouchy, and C. Moutou

Multiplicity-study of exoplanet host stars

M. Mugrauer[1], R. Neuhäuser[1], T.Mazeh[2], and E. Guenther[3]

[1] *Astrophysikalisches Institut, Universität Jena, Schillergäßchen 2-3, 07745 Jena, Germany [markus@astro.uni-jena.de]*

[2] *Tel Aviv University, Tel Aviv 69978, Israel*

[3] *Thüringer Landessternwarte Tautenburg, Sternwarte 5, 07778 Tautenburg, Germany*

Abstract. We carry out a systematic search campaign for wide companions of exoplanet host stars to study their multiplicity and its influence on the long-term stability and the orbital parameters of the exoplanets. We have already found 6 wide companions, raising the number of confirmed binaries among the exoplanet host stars to 20 systems. We have also searched for wide companions of Gl 86, the first known exoplanet host star with a white dwarf companion. Our Sofi/NTT observations are sensitive to substellar companions with a minimum-mass of 35 M_{Jup} and clearly rule out further stellar companions with projected separations between 40 and 670 AU.

1. An imaging search campaign for wide companions of exoplanet host stars

Some of the exoplanet host stars were found to be components of binary systems and first statistical differences between exoplanets around single stars and exoplanets located in binary systems were already reported by Zucker & Mazeh (2002) as well as Eggenberger et al. (2004). In particular, it seems that planets with orbital periods shorter than 40 days exhibit a difference in their mass-period and eccentricity-period distribution.

However, all the derived statistical differences are based only on a small number of known binary systems among the exoplanet host stars, i.e. their significance is sensitive to any changes in the sample size.

Furthermore in the statistical analyses it is assumed that most of the exoplanet host stars are single star systems expect these stars known to be a component of a binary system.

In that context it is important to mention that the whole sample of exoplanet host stars was not systematically surveyed so far for neither wide nor close companions, i.e. several more exoplanet host stars, considered today as single stars, might be members of binary systems. Only search campaigns for companions of the exoplanet host stars will clarify their multiplicity status and will finally verify the significance of the reported statistical differences.

Therefore, we have started an imaging search program for wide visual companions of exoplanet host stars, carried out with UFTI/UKIRT, SofI/NTT as well as MAGIC/CA 2.2m. We can find all directly detectable stellar and substellar companions ($m \gtrsim 40\,M_{Jup}$) with projected separations from about 50 up to 1000 AU. Thereby companions are identified first with astrometry (common proper motion) and their companionship is confirmed with photometry and spectroscopy later on. So far, 6 wide companions were detected, see Mugrauer et al. (2005a) for further details.

2. Gl 86 B, a white dwarf companion of an exoplanet host star

Queloz et al. (2000) reported a long-term linear trend in the radial velocity of the exoplanet host star Gl 86. Furthermore, after combining Hipparcos measurements with ground-based astrometric catalogues, Jahreiß (2001) showed that this star is a highly significant $\Delta\mu$ binary. Both results point out that there should be a companion of stellar mass in orbit around Gl 86. Els et al. (2000) indeed detected a faint common proper motion companion, Gl 86 B, with a separation of only ~ 2 arcsec and concluded that it is a late L or early T brown dwarf.

With NACO/SDI observations, Mugrauer & Neuhäuser (2005b) detected the orbital motion of this companion which is the final proof that it is orbiting the exoplanet host star. Furthermore they showed with IR spectroscopy data that Gl 86 B is a white dwarf, i.e. this companion is the causer of the reported linear trends in the radial and astrometric motion of the exoplanet host star. Gl 86 B is the first known white dwarf detected as a close companion of an exoplanet host star. With their high contrast NACO/SDI imaging, Mugrauer & Neuhäuser (2005b) can already exclude further stellar companions around Gl 86 with projected separations between 1 and 23 AU.

We present here further complementary observations of the Gl 86 binary system, carried out in our wide companion search program using

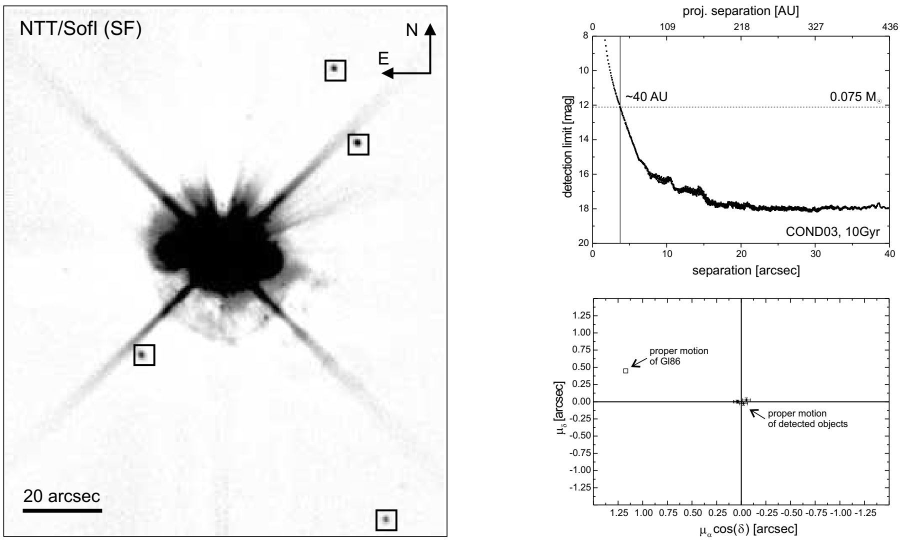

Figure 1. *The left panel shows the 1st epoch H-band image of Gl 86 obtained with SofI/NTT in Dec. 2002. We observed the star again in 2nd epoch in June 2003. A detection limit of H=18 mag (S/N=10) is reached and substellar companions with a minimum-mass of 35* M_{Jup} *are detectable (see right upper plot). The proper motion between the 1st and 2nd epoch imaging of all detected objects is illustrated in the right lower diagram.*

SofI/NTT. With these observations, we can clearly rule out additional wide stellar companions around Gl 86 with projected separations between 40 and 670 AU (see Fig. 1).

References

Eggenberger A., Udry S., & Mayor M., 2004, A&A, 417, 353

Els S. G., Sterzik, M. F., Marchis F., et al., 2001, A&A, 370, 1

Jahreiß H., 2001, AGM, 18, 110

Mugrauer M., Neuhäuser R., Seifahrt A., et al., 2005a, A&A, 440, 1051

Mugrauer M. & Neuhäuser R., 2005b, MNRAS, 361, 15

Queloz D., Mayor M., Weber L., et al., 2000, A&A, 354, 99

Zucker S. & Mazeh T., 2002, ApJ, 568, 113